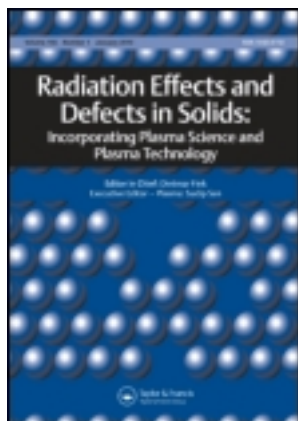


This article was downloaded by: [Balikesir University]

On: 14 December 2012, At: 02:44

Publisher: Taylor & Francis

Informa Ltd Registered in England and Wales Registered Number: 1072954 Registered office: Mortimer House, 37-41 Mortimer Street, London W1T 3JH, UK



Radiation Effects and Defects in Solids: Incorporating Plasma Science and Plasma Technology

Publication details, including instructions for authors and subscription information:

<http://www.tandfonline.com/loi/grad20>

Determination of dosimetric and kinetic features of gamma irradiated solid calcium ascorbate dihydrate using ESR spectroscopy

H. Tuner^a

^a Department of Physics, Faculty of Science, Balikesir University, 10145, Cagis, Balikesir, Turkey

Version of record first published: 01 Oct 2012.

To cite this article: H. Tuner (2013): Determination of dosimetric and kinetic features of gamma irradiated solid calcium ascorbate dihydrate using ESR spectroscopy, Radiation Effects and Defects in Solids: Incorporating Plasma Science and Plasma Technology, 168:1, 61-71

To link to this article: <http://dx.doi.org/10.1080/10420150.2012.729585>

PLEASE SCROLL DOWN FOR ARTICLE

Full terms and conditions of use: <http://www.tandfonline.com/page/terms-and-conditions>

This article may be used for research, teaching, and private study purposes. Any substantial or systematic reproduction, redistribution, reselling, loan, sub-licensing, systematic supply, or distribution in any form to anyone is expressly forbidden.

The publisher does not give any warranty express or implied or make any representation that the contents will be complete or accurate or up to date. The accuracy of any instructions, formulae, and drug doses should be independently verified with primary sources. The publisher shall not be liable for any loss, actions, claims, proceedings, demand, or costs or damages whatsoever or howsoever caused arising directly or indirectly in connection with or arising out of the use of this material.

Determination of dosimetric and kinetic features of gamma irradiated solid calcium ascorbate dihydrate using ESR spectroscopy

H. Tuner*

Department of Physics, Faculty of Science, Balikesir University, 10145 Cagis, Balikesir, Turkey

(Received 1 March 2012; final version received 3 September 2012)

Effects of gamma radiation on solid calcium ascorbate dihydrate were studied using electron spin resonance (ESR) spectroscopy. Irradiated samples were found to present two specific ESR lines with shoulder at low and high magnetic field sides. Structural and kinetic features of the radicalic species responsible for experimental ESR spectrum were explored through the variations of the signal intensities with applied microwave power, variable temperature, high-temperature annealing and room temperature storage time studies. Dosimetric potential of the sample was also determined using spectrum area and measured signal intensity measurements. It was concluded that three radicals with different spectroscopic and kinetic features were produced upon gamma irradiation.

Keywords: ESR; calcium ascorbate; irradiation; radical; kinetic

1. Introduction

Calcium ascorbate dihydrate (CaAs), or chemically calcium salt of 2,3-didehydro-L-threohexono-1,4-lactone dihydrate, is water soluble calcium salt of ascorbic acid (AAs), and has the formula of $\text{Ca}[(\text{C}_6\text{H}_7\text{O}_6)^-]_2 \cdot 2\text{H}_2\text{O}$. CaAs is white to slightly yellow odorless crystalline powder with a melting point about 440 K. It crystallizes as the monoclinic with the space group of $P2_1$ and there are two molecules in the unit cell (1–3). It is commonly used in food and cosmetic industries as an antioxidant (4–8) and in medicine as vitamin C and Ca source (9–12). CaAs is a common antibrowning agent for several fresh-cut fruits, primarily for apples (13–19).

Using ionizing radiation for sterilization of foods and pharmaceuticals has been established as a safe and effective method after more than five decades of research and development. High penetrating power, low measurable residues, small temperature rise and fewer variables to control are the advantages of the radiosterilization. Thus, sterilization can be carried out on the finally packaged product and is applicable to heat-sensitive products (20–23). Despite these advantages, irradiation also causes damage in the molecular structure. Electron spin resonance (ESR) spectroscopy has been frequently used for identifying irradiation damage centers in many substances

*Email: htuner@balikesir.edu.tr; htuner@hacettepe.edu.tr

(24–32). In this study, kinetic and structural features of the radicalic intermediates produced upon gamma irradiation and dosimetric features of CaAs were studied using ESR spectroscopy.

Effects of gamma radiation on AAs and its sodium salt (NaAs) have been reported by different researchers using ESR spectroscopy (26–32). Rexroad and Gordy (26) have already reported the gamma radiation effects on solid CaAs, and they observed a singlet ESR line. However, room- and high-temperature kinetic features, and spectroscopic parameters of the radical species produced after irradiation of CaAs were not reported in the literature. Therefore, the aim of this study is to determine the room- (290 K) and high-temperature (370, 380, 390 and 400 K) kinetic features, structures and spectroscopic parameters of the radical species produced upon gamma irradiated CaAs through annealing studies and spectrum simulation calculations, respectively. Moreover, the usefulness of ESR spectroscopy in determining the applied radiation dose to CaAs is investigated.

2. Materials and methods

CaAs sample was provided from Aldrich and used without any further treatment by keeping in sealed polyethylene vials at room temperature (290 K) before irradiation. All irradiations and ESR experiments were carried out at room temperature and on samples open to air in order to stay under commercial food irradiation and radiation sterilization conditions, and to explore the possible dosimetric use of CaAs as a normal and/or accidental dosimeter. The irradiations were performed using a ^{60}Co - γ source supplying a dose rate of 0.8 kGy/h. Dose–response curves were obtained using a set of samples irradiated at doses of 0.5, 1.0, 2.0, 5.0, 7.0, 10.0, 15.0 and 20.0 kGy. Samples irradiated to a dose of 10 kGy were used to investigate structural, spectral and kinetic features of the contributing radical species.

ESR measurements were carried out on samples transferred into quartz ESR tubes of 4 mm inner diameter, using a Bruker EMX-131 X-band ESR spectrometer operating at 9.8 GHz and equipped with high-sensitive cylindrical cavity. The operation conditions for both room/high and low temperatures were determined from the microwave power investigations derived at room (290 K) and low (130 K) temperatures, and modulation amplitude investigations were derived at room temperature (central field, 351.5 mT; microwave power, 0.32 mW; microwave frequency, ~ 9.86 GHz; (central field, 334.7 mT; microwave power, 0.02 mW; receiver gain, 2.52×10^4 ; microwave frequency, ~ 9.39 GHz at low temperatures), scan range, 6 mT; modulation amplitude, 0.1 mT; receiver gain, 1.00×10^4 ; modulation frequency, 100 kHz; sweep time, 83.89 s). Signal intensities were measured directly from the experimental spectra, and the spectrum area under absorption curves, which is proportional to the total number of the produced radicals, was calculated by the double integration technique using the Bruker WINEPR program (33).

The sample temperature was controlled using Bruker ER 411-VT digital temperature control unit. Cooling, heating and subsequent cooling cycles were adopted to monitor free-radical signal evaluations over a large temperature range. The temperature of the samples was first decreased to 130 K, starting from room temperature with a decrement of 20 K, then increased to 400 K and finally decreased again to room temperature. Kinetic behaviors of the involved radical species were evaluated at four different temperatures (370, 380, 390 and 400 K). The samples were heated to a predetermined temperature and kept at this temperature for about 5 min; then, spectra were recorded at intervals of 2 min without cooling samples to room temperature.

3. Experimental results and discussion

Irradiated CaAs was observed to present an ESR spectrum consisting of two main strong resonance lines (Figure 1). The spectrum that observed for gamma irradiated CaAs is quite different from that

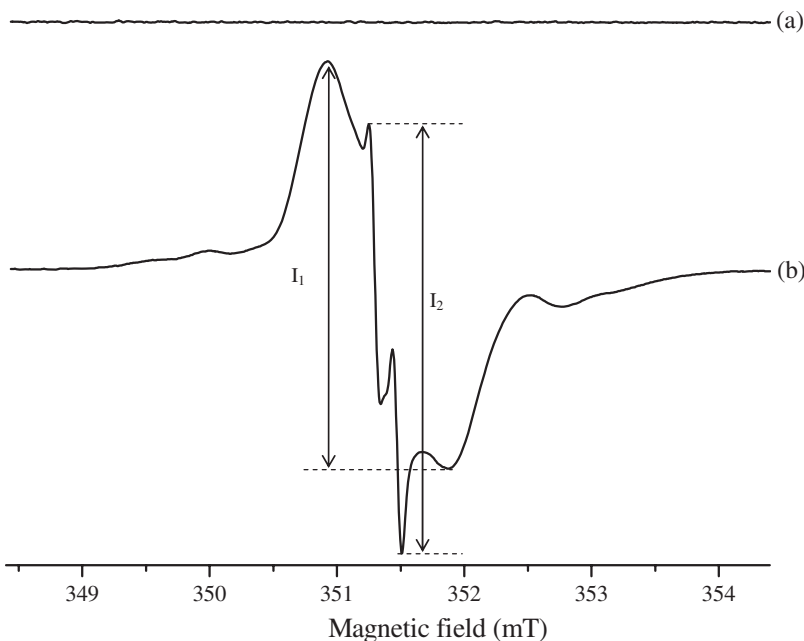


Figure 1. ESR spectra of CaAs: (a) unirradiated and (b) irradiated at 10 kGy.

reported by Rexroad and Gordy (26). Room temperature spectra were calculated to spread over a magnetic field range 5 mT and centered at about $g = 2.0052$. The main strong broad line (I_1) is a singlet or unresolved doublet and the other strong line (I_2) that located almost at the middle of the spectra has a small hyperfine splitting with narrow linewidth (~ 0.1 mT). These narrow linewidth make it possible to distinguish the doublet separately. The ESR spectra of irradiated CaAs also have very weak lines that located at both sides of the strong lines (Figure 1(b)). Although evaluation of these weak lines was not possible, the spectroscopic features of the responsible radical were determined by spectrum simulation calculations. These preliminary investigations predict the presence of two or three different radicals upon irradiation CaAs.

3.1. Variations of the signal intensities with microwave power and modulation amplitude

Samples irradiated at a dose of 10 kGy were used to determine the microwave power saturation features of the associated radical species. Variations of the assigned line intensities with microwave power were investigated both at room temperature (290 K) and at 130 K in the ranges 6.40×10^{-4} – 6.36 and 2.00×10^{-4} – 0.50 mW, respectively. The measured lines exhibited the characteristic behavior of homogeneously broadened resonance lines at room temperatures, that is, an increase at low powers, and then a decrease at high powers. At low temperature (130 K), the monitored ESR lines were shown as an inhomogeneously broadened resonance lines. However, evaluation of I_2 was not possible due to the screening of I_1 . The results are given in Figure 2.

Effects of the modulation amplitude on the ESR lines were also investigated. To achieve this goal, the sample irradiated at 10 kGy and 0.32 mW microwave power value was recorded at room temperature at different modulation amplitudes. Variations of each ESR lines of irradiated CaAs in the range 0.02–0.25 mT are given in Figure 3. Although high modulation amplitudes increase the signal intensities, the resolution is not as good as at low modulation amplitudes. Thus, 0.10 mT is accepted as the modulation amplitude value in this study.

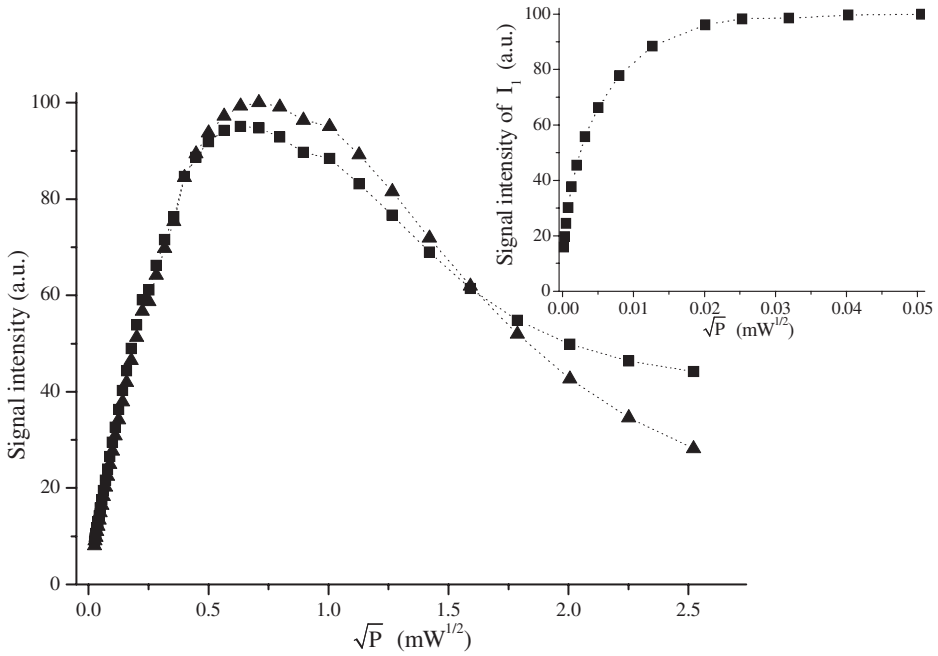


Figure 2. Microwave saturations at room temperature for I_1 (■) and I_2 (▲) intensities for a sample irradiated at a dose of 10 kGy. Inset: microwave saturations at 130 K.

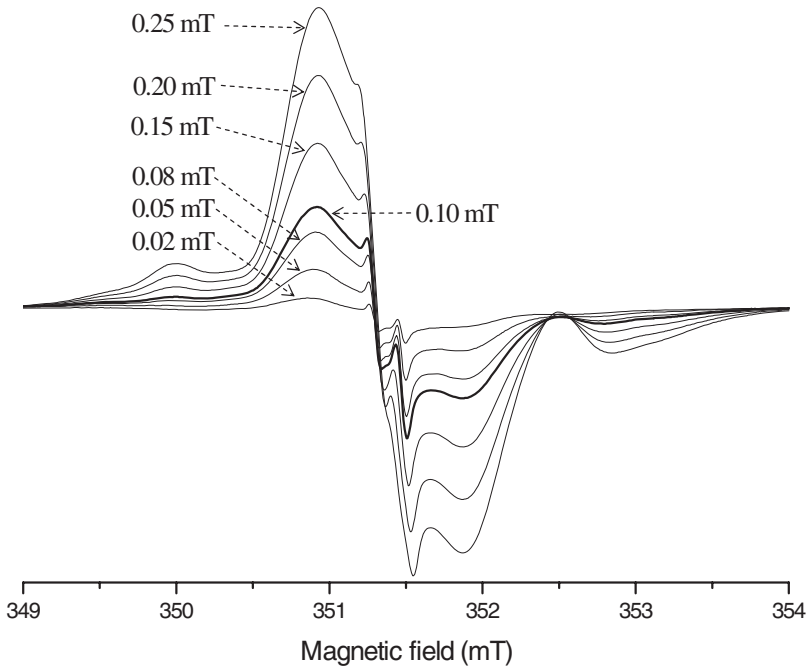


Figure 3. Variations of ESR spectra of CaAs irradiated to a dose of 10 kGy with applied modulation amplitudes at the microwave power of 0.32 mW.

Table 1. Mathematical functions, parameter values and correlation coefficient best describing experimental dose–response data.

Functions		Spectrum area	I_1	I_2
$I = a + b \times D + c \times D^2$	a	12.769	3.673	21.118
	b	32.000	8.665	8.121
	c	−0.642	−0.193	−0.239
	r^2	0.9978	0.9987	0.9577
$I = h \times D^j$	h	52.655	14.857	31.226
	j	0.685	0.651	0.368
	r^2	0.9947	0.9918	0.9744
$I = k \times (1 - e^{-m \times D})$	k	503.436	120.197	84.950
	m	0.077	0.090	0.298
	r^2	0.9979	0.9978	0.9806
$I = n \times (1 - e^{-p \times D}) + q \times (1 - e^{-s \times D})$	n	435.060	84.730	84.772
	p	0.085	0.106	0.042
	q	231.569	43.189	44.318
	s	0.010	0.046	0.904
	r^2	0.9978	0.9977	0.9837

3.2. Dose–response curves

ESR spectroscopy is commonly used for dose measurement and the discrimination of irradiated samples from unirradiated ones. For this purpose, the best mathematical functions used to describe the dose–response curves should be determined. Linear, polynomial and exponential functions are frequently used for this purpose (27–32). Samples irradiated at dose range 0.5–20.0 kGy were used to construct dose–response curves. Measured signal intensities and calculated spectrum area from recorded spectra were normalized to the mass of samples and spectrometer gain. Mathematical functions given in Table 1 were tried to fit the experimental dose–response data in this study. It was concluded that an exponential function of applied dose, that is, a function of the type $I = k \cdot (1 - e^{-m \cdot D})$ describes best experimental data, where I and D stand for intensity/spectrum area and applied dose in kilogray, respectively. The results are presented in Figure 4.

The weak lines, which located at both side of the main strong lines, are hardly distinguishable at low radiation doses, and slightly start to distinguish at high radiation doses.

3.3. Variable temperature studies

Changes in the signal intensities with temperature can give novel information concerning the stabilities and the number of radical types created upon irradiation. Variations of the monitored I_1 intensity (Figure 1(b)) and spectrum area with temperature were investigated in the temperature range 130–400 K using a sample irradiated to a dose of 10 kGy. To avoid saturation even at the lowest temperature achievable in this study (130 K), care was taken with the use of microwave power. Cooling the sample to 130 K produced similar continuous increases in all intensities. The variations of spectrum area, which is proportional to the total numbers of the produced radicals, and the dominant line intensity (I_1) are illustrated in Figure 5. The intensities and the spectrum area were normalized to their value at 130 K. The decrease on the increment rate at low temperature was concluded to be from the microwave saturation effect. The high increment rate of the broad strong line I_1 makes it difficult to evaluate the variations of the I_2 intensity below room temperature.

Heating the sample again to room temperature shows a reversible change, and the measured intensity and spectrum area reached to their initial values before cooling. Heating the sample

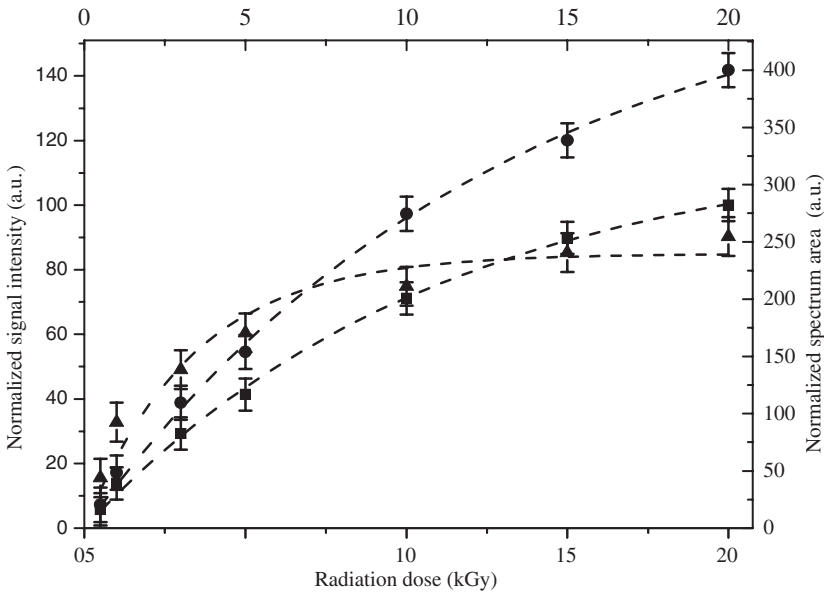


Figure 4. Variations of the measured intensities and spectrum area with applied radiation dose. Symbols: experimental (spectrum area (●); I_1 (■); I_2 (▲)); lines: calculated using an exponential function.

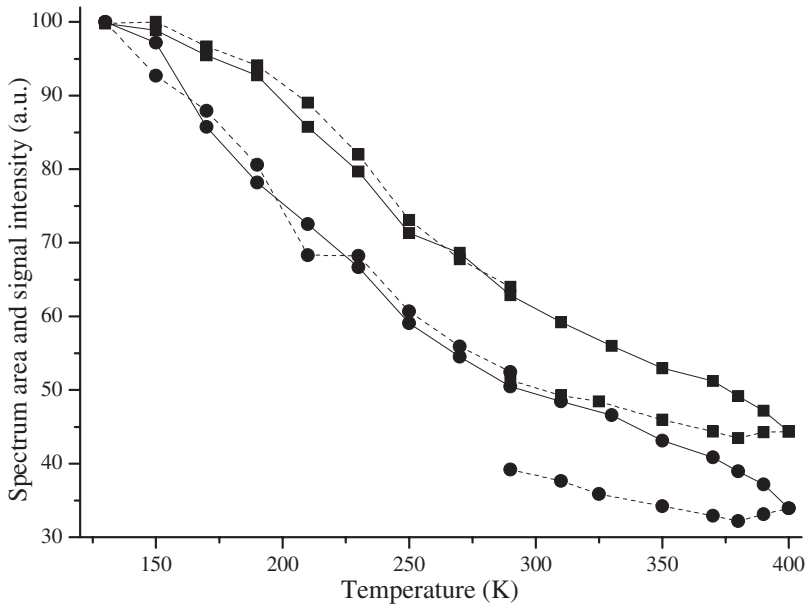
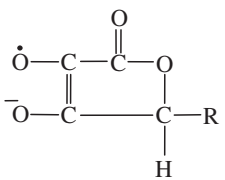
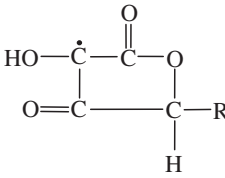


Figure 5. Variations of the spectrum area (●) and I_1 (■) with temperature for a sample irradiated at a 10 kGy. (Cooling: 290 \rightarrow 130 K and 400 \rightarrow 290 K (dashed lines); heating 120 \rightarrow 400 K (solid lines)).

above room temperature produced irreversible decreases in the investigated intensity (I_1) and spectrum area (Figure 5). However, the decay rates in the signal intensities and spectrum area were not the same. The spectrum area decreases faster than intensity I_1 . This observation predicts the presence of more than one radical species upon irradiation of CaAs.

Table 2. Spectroscopic parameters calculated for contributing radical species.

Radical	Relative weight	Linewidth ΔH_{pp} (mT)	g -Value	Hyperfine splitting (mT)
 (R1)	84.04 ± 1.73	0.703 ± 0.021	2.0056 ± 0.0004	–
 (R2)	3.35 ± 0.84	0.105 ± 0.028	2.0051 ± 0.0006	0.161 ± 0.015
$\dot{\text{C}}\text{H}^1\text{OH}^2\text{CH}_2\text{OH}$	12.61 ± 1.19	0.196 ± 0.018	2.0046 ± 0.0003	H^1 1.467 ± 0.009 H^2 0.823 ± 0.008

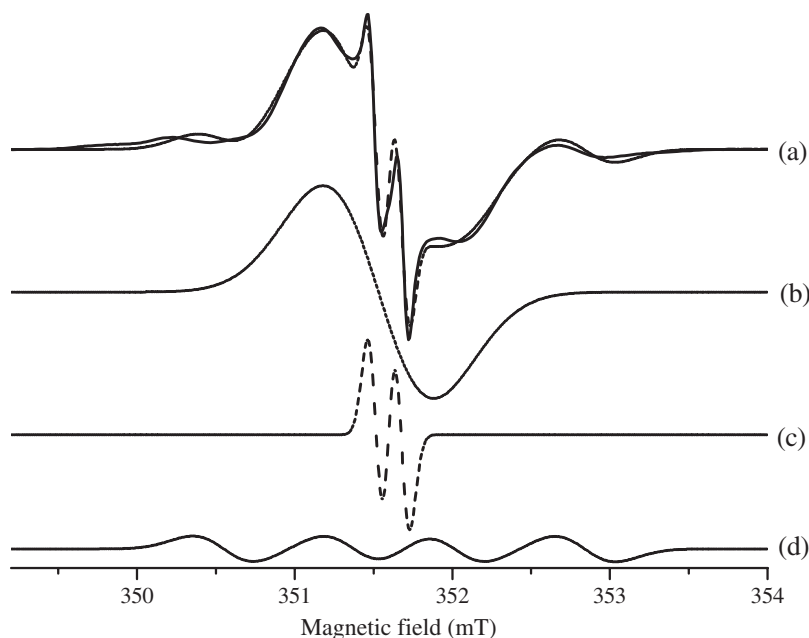


Figure 6. Experimental (solid line) and theoretical (dashed line) ESR spectra calculated using parameter values given in Table 2. Sum spectra (a) and spectra of each radical (R1 (b), R2 (c), R3 (d)).

3.4. Simulation and proposed tentative radical species

Spectrum simulation basing on two models predicting the presence of two and three radical species with different spectroscopic features were tried separately to determine the experimental spectrum of gamma irradiated CaAs. Predicting the presence of three radical species was found to be the best model that describes the experimental spectrum. Signal intensity data derived from room temperature ESR spectra of a sample irradiated at a dose of 10 kGy were used. The results of the

Table 3. Decay constants and activation energies calculated for responsible radical species at four different annealing temperatures.

Species	Decay constants ($\text{min}^{-1} \times 10^{-3}$)				Activation energy (kJ/mol)
	370 K	380 K	390 K	400 K	
R1	1.56	2.86	5.98	9.80	75.79 ± 1.32
R2	39.57	61.67	110.76	163.14	59.28 ± 0.73
R3	5.62	16.65	56.04	120.40	120.65 ± 9.74

simulations are presented in Table 2. Theoretical spectrum of each species and their sum were also given in Figure 6 with their experimental counterpart for comparison. It is seen that theoretical and experimental spectra are in good agreement and that model based on the presence of three different radical species of different kinetic and spectroscopic features describes the experimental spectrum very well. According to the spectroscopic features derived from the spectrum simulations, these three radicals showed similar features to the radicals which were previously proposed for irradiated CaAs (26), AAs (26, 29–31) and NaAs (32). The radical proposed by Rexroad and Gordy (26), which was produced by loss of the hydroxyl H atom and did not show any hyperfine splitting, is the radical responsible for the main strong singlet line (I_1), and it is denoted as radical R1 in this study. The other radical proposed by Tüner and Korkmaz (29, 31) and denoted as radical-II for AAs and radical-A for NaAs is the radical responsible from the doublet which located at the middle of the broad line (denoted as R2 in this study). The radical denoted as radical-I by Tüner and Korkmaz (30) which proposed to be produced after gamma irradiation of AAs and has the form of CHOHCH_2OH (R3 in this study) is also produced in gamma irradiated CaAs. The unpaired electron of the latter radical interacts with two inequivalent protons, which cause to split to four ESR lines.

3.5. Annealing studies at high temperature

Variations of the line intensities and spectrum area at high temperature were studied to get information about kinetic features of the radicals produced in irradiated CaAs. Data derived at four different temperatures (370, 380, 390 and 400 K) for the spectrum area of a sample irradiated at 10 kGy are given in Figure 7. Similar variations were obtained for the measured line intensities (I_1 and I_2). Due to difficulties in determining the contribution ratio of each radical to the signal intensities, calculated spectrum area is used in this investigation. Therefore, the relative weight that obtained from the spectrum simulation for each radical could be used to get a better result about the kinetics of the radicals. A function of the type of $Y(t) = Y_{(R1)0} \cdot \exp(-k_{R1} \cdot t) + Y_{(R2)0} \cdot \exp(-k_{R2} \cdot t) + Y_{(R3)0} \cdot \exp(-k_{R3} \cdot t)$ was used to fit the experimental decay data, where $Y_{(R)0}$'s indicates the initial radical weights, and k_R 's indicates the decay constants to be determined. The results obtained for the spectrum area are given in Table 3. Calculated decay constants given in the table were used to drive theoretical variation curves of the calculated spectrum area data with annealing time at each annealing temperature. Activation energies of the radicals were calculated from $\ln(k) - T^{-1}$ graphs (Arrhenius graph) and following values were obtained for each radical; $E_{R1} = 75.79$ kJ/mol, $E_{R2} = 59.28$ kJ/mol and $E_{R3} = 120.65$ kJ/mol.

3.6. Stability of the radical at room temperature

The sample irradiated at a dose of 10 kGy was stored at room temperature open to air over a storage period of 90 days and its spectra were recorded in regular time intervals. Collected data relevant

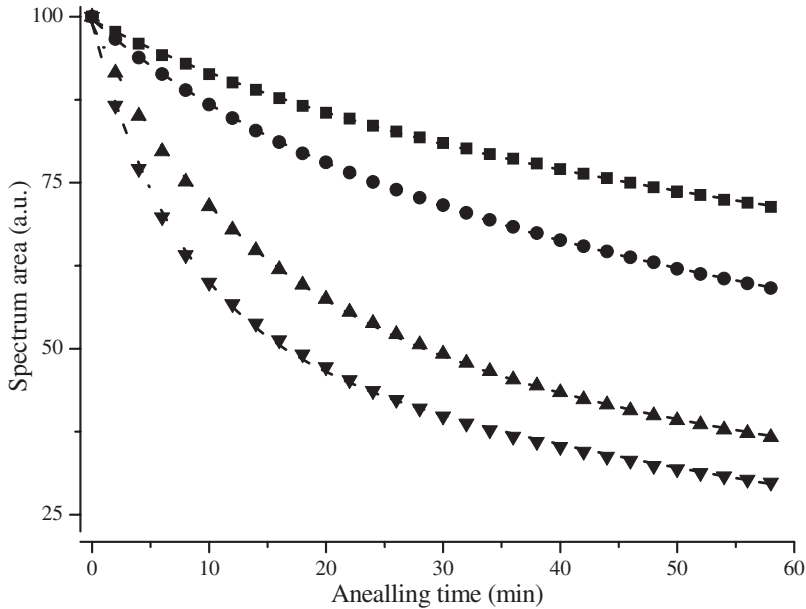


Figure 7. Variations of the spectrum area for a sample irradiated at dose of 10 kGy with annealing time at four different temperatures. Symbols: experimental (370 K (■), 380 K (●), 390 K (▲) and 400 K (▼)); lines: theoretical (calculated using parameters given in Table 3).

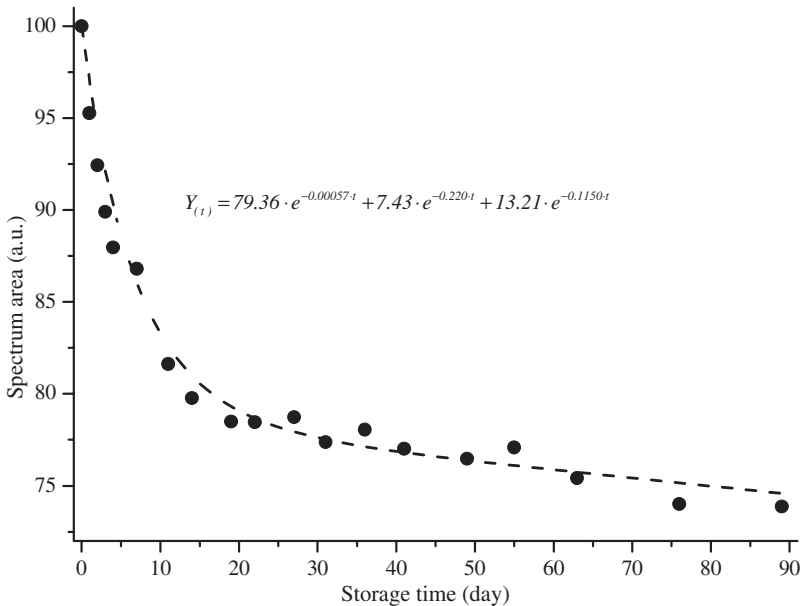


Figure 8. Variation of the spectrum area with storage time at room temperature.

to the spectrum area are presented in Figure 8. As it is seen, the spectrum area experiences fast decreases at the beginning of the storage period and after 2 weeks, more than 20% were decayed.

In agreement with the results of the spectrum simulation and annealing at high temperature studies and with the literature findings on irradiated CaAs and AA (26, 30), three radical species

having different decay characteristics were predicted to take part in the formation of the experimental ESR spectrum of gamma irradiated CaAs. The measured room temperature decay data of the spectrum area were fitted to the same function, which was used in the annealing study. These functions present the characteristics of the first-order decay kinetics, and t is the time elapsed after stopping irradiation.

4. Conclusions

Gamma irradiated CaAs exhibits an ESR spectrum with many resonance lines, which can be classified into three subgroups; (i) strong singlet with broad linewidth, (ii) doublet with weak linewidth and (iii) weak lines located at both sides of the strong lines. A model based on the presence of three radical species, denoted as R1, R2 and R3 of different spectroscopic and kinetic features, was found to describe the experimental spectra well. Rexroad and Gordy (26) previously proposed the radical R1 produced in irradiated CaAs, and the radicals R2 and R3 were proposed by Tüner and Korkmaz (30, 32) for AAs and NaAs salts. The same radicalic species but with slightly different spectroscopic features are predicted to be produced in the gamma irradiated CaAs.

The decay of assigned lines and spectrum area above room temperature are relatively fast. Above 380 K, decrease in the intensity of I_2 is faster than I_1 and at the end of the annealing times at 400 K, its maximum start is to be screened by the broad strong line. It is concluded that the radical R2 decay faster than radical R1. At room temperature almost 20% of the total amount of radicals were decayed after 2 weeks of irradiation. Despite all these negative findings from decay at room and high temperatures, ESR spectroscopy could be used for the discrimination of irradiated CaAs from unirradiated one even after a storage period of 3 months.

References

- (1) Hvoslef, J.; Kjellef, K.E. *Acta Cryst. B* **1974**, *30*, 2711–2716.
- (2) Hearn, R.A.; Bugg, C.E. *Acta Cryst. B* **1974**, *30*, 2705–2711.
- (3) Abrahams, S.C.; Bernstein, J.L.; Bugg, C.E.; Hvoslef, J. *Acta Cryst. B* **1978**, *34*, 2981–2985.
- (4) Wenninger, J.A.; Canterbury, R.C.; McEwen, G.N. Jr., Eds. *International Cosmetic Ingredient Dictionary and Handbook*, 8th ed.; Washington, DC: Cosmetic, Toiletry, and Fragrance Association, 2000; 1–2 vols.
- (5) Andersen, F.A. *Int. J. Toxicol.* **2005**, *24*, 51–111.
- (6) Gönüllü Ü.; Yener, G.; Üner, M.; Incegil, T. *Int. J. Cosmet. Sci.* **2004**, *26*, 31–36.
- (7) Scientific Opinion of the Panel on Food Additives and Nutrient Sources added to Food on a request from the Commission on magnesium ascorbate, zinc ascorbate and calcium ascorbate added for nutritional purposes in food supplements. *J. EFSA* **2009**, *994*, 1–22.
- (8) European Food Safety Authority; Safety of calcium ascorbate with a content of threonate produced by a new manufacturing process as a source of vitamin C in food supplements. *J. EFSA* **2011**, *9*, 2395–2412.
- (9) Bush, M.J.; Verlangieri, A.J. *Res. Commun. Chem. Pathol. Pharmacol.* **1987**, *57*, 137–140.
- (10) Hiatt, A.N.; Ferruzzi, M.G.; Taylor, L.S.; Mauer, L.J. *Int. J. Food Prop.* **2011**, *14*, 1330–1348.
- (11) Balch, J.; Balch, P. *Prescription for Nutritional Healing*, 2nd ed.; Garden City Park, Avery Publishing Group, 1997.
- (12) Cai, J.; Zhang, Q.; Wastney, M.E.; Weaver, C.M. *Exp. Biol. Med.* **2004**, *229*, 40–45.
- (13) Chen, C.; Trezza, T.A.; Wong, D.W.S.; Camir, W.M.; Pavlath, A.E., inventors; Mantrose-Hauser Co. Inc. Methods for Preserving Fresh Fruit and Product Thereof. Assignee. US patent 5,939,117, August 17, 1999.
- (14) Karabrahimoglu, Y.; Fan, X.; Sapers, G.M.; Sokorai, K.J.B. *J. Food Protect.* **2004**, *67*, 751–757.
- (15) Fan, X.; Sokorai, K.J.B.; Sommers, Ch.H.; Niemira, B.A.; Mattheis, J.P. *J. Food Sci.* **2005**, *70*, M352–M358.
- (16) Fan, X.; Niemira, B.A.; Mattheis, J.P.; Zhuang, H.; Olson, D.W. *J. Food Sci.* **2005**, *70*, S143–S148.
- (17) Fan, X.; Sokorai, K.J.B. *J. Food Sci.* **2008**, *73*, C79–C83.
- (18) Wang, H.; Feng, H.; Luo, Y.J. *Food Sci.* **2007**, *72*, M1–M7.
- (19) Aguayo, E.; Requejo-Jackman, C.; Stanley, R.; Woolf, A. *Postharvest Biol. Tec.* **2010**, *57*, 52–60.
- (20) Desrosiers, M.F. *Appl Radiat Isot.* **1996**, *47*, 1621–1628.
- (21) Desrosiers, M.F.; Ostapenko, T.; Puhl, J.M. *Radiat. Phys. Chem.* **2009**, *78*, 457–460.
- (22) Korkmaz, M.; Polat, M. In *Improving the Safety of Fresh Fruit and Vegetables*; Jongon, W., Ed., Woodhead Publishing Limited, Cambridge, UK, 2005, pp 387–428.

- (23) Chimbombi, E.; Moreira, R.G.; Kim, J.; Castell-Perez, E.M. *J. Food Eng.* 2011, *103*, 409–416.
- (24) Maghraby, A.; Salama, E.; Sami, A.; Mansour, A.; El-Sayed, M. *Radiat. Eff. Def. Solids* **2012**, *167*, 170–178.
- (25) Merdan, M.A.; Aşik, B.; Birey, M.; Aras, E. *Radiat. Eff. Def. Solids*. **2012**, *167*, 179–183.
- (26) Rexroad, H.N.; Gordy, W. *Proc. Natl. Acad. Sci.* **1959**, *45*, 256–269.
- (27) Basly, J.P.; Longy, I.; Bernard, M. *Pharm. Res.* **1997**, *14*, 1186–1191.
- (28) Basly, J.P.; Basly, I.; Bernard, M. *Anal. Chim. Acta.* **1998**, *372*, 373–378.
- (29) Polat, K.; Korkmaz, M. *Anal. Chim. Acta.* **2005**, *535*, 331–337.
- (30) Tuner, H.; Korkmaz, M. *J. Radioanal. Nucl. Chem.* **2007**, *273*, 609–614.
- (31) Tuner, H.; Korkmaz, M. In *Proceedings of the 6th International Conference of the Balkan Physical Union*, AIP Conference Proceedings, Istanbul, Turkey, August 22–26, 2007; Cetin, S.A.; Hikmet, I., Eds; 899, 570, 2007.
- (32) Tuner, H.; Korkmaz, M. *Radiat. Eff. Defects Solids* **2008**, *163*, 95–105.
- (33) Barr, D.; Jiang, J.J.; Weber, R. *Performing Double Integrations using WIN-EPR*; Bruker biospin report 6, 1998. Available from <http://www.brukerbiospin.com/brukerepr/pdf/doubleint.pdf>